Applied Surface Science 543 (2021) 148557

Contents lists available at ScienceDirect

Applied Surface Science

journal homepage: www.elsevier.com/locate/apsusc

Full Length Article

Dissociative chemisorption of methyl fluoride and its implications for atomic layer etching of silicon nitride

Erik Cheng [a], Gyeong S. Hwang [a,b,*]

[a] Texas Materials Institute, The University of Texas at Austin, Austin, TX 78712, USA
[b] McKetta Department of Chemical Engineering, The University of Texas at Austin, Austin, TX 78712, USA

ARTICLE INFO

Keywords:
Atomic Layer Etching
Silicon nitride
Methyl fluoride
Density functional theory calculation

ABSTRACT

Atomic layer etching (ALE) of silicon nitride with sequential exposure to hydrofluorocarbons and low energy ion bombardment has been demonstrated. The ALE mechanism is generally thought to consist of surface modification via hydrofluorocarbon chemisorption followed by removal of the chemically modified surface layer by ion bombardment, but the underlying details are not fully understood. Using first-principles calculations, we have examined a possible pathway for dissociative chemisorption of CH_3F and assessed its potential role in Si_3N_4 ALE. According to our results, the initial sticking probability tends to be very low ($<10^{-7}$) even on the H-terminated N-rich surface that is the most reactive towards CH_3F, in the absence of dangling bonds. Furthermore, the chemisorption does not significantly modify the strength of surface Si-N bonds or yield a stoichiometrically reasonable pathway for the etching of a full atomic layer. Our findings suggest that reactive species generated from CH_3F dissociation and surface activation induced by Ar^+ ion bombardment can be key factors in achieving ALE of Si_3N_4 with CH_3F, in contrast to the common explanation of surface chemical modification via direct reaction with CH_3F.

1. Introduction

As semiconductor manufacturing continues to push into (and beyond) the sub-10 nm node [1] in efforts to keep pace with Moore's Law, it has become of great importance to achieve increasingly finer levels of control over etch variability [2–4]. Conventional methods, such as reactive ion etching (RIE), can be damaging and uncontrollable [5,6]. The need for gentler etch methods with finer achievable resolution has spurred research into more advanced techniques, including atomic layer etching (ALE) [3,4,6]. This technique, first developed in 1988, [7] has attracted interest within recent years due to its promised ability to deliver monolayer scale precision in etching [3,4].

The ALE process generally consists of two alternating steps which are repeated until the desired etch amount is achieved, with each two-step cycle ideally removing one atomic layer of material [7]. The first step is designed to chemically activate the surface, where a precursor is thought to react with the top layer of substrate to create a chemically modified surface layer. In principle, this should render the surface susceptible to selective etch. The surface activation step is then followed by a removal step, often achieved through plasma bombardment of the surface, [8,9] to etch away the activated surface layer of the substrate. The nature of surface chemical modification, if achieved, is largely responsible for the self-limiting property of ALE; in the ideal process, excess precursor will not react further once the surface layer is completely saturated, producing an etch with atomic layer resolution.

Recently, Kim *et al.* demonstrated that ALE of silicon nitride (Si_3N_4) could be achieved using a CH_3F precursor followed by Ar^+ bombardment [10]. Their controlled ALE process achieved an etch depth of about 6 Å per cycle after precursor saturation in each cycle, corresponding to one atomic layer removed per cycle. The successful ALE of Si_3N_4 is of great importance due to the myriad applications of Si_3N_4 in semiconductor manufacturing, [11,12] where the ability to control its etching with atomic layer precision has become critically important in recent years. However, there is still a fundamental lack of understanding of the underlying mechanism responsible for the ALE of Si_3N_4 with CH_3F. Experimental and computational studies have been undertaken to examine similar processes, such as etching via F atoms [13] and the wet chemical etching with HF-based solutions, [14] but are insufficient to explain the gas/surface chemistry occurring in this ALE process.

This work intends to explore the role of CH_3F in Si_3N_4 ALE. We first

* Corresponding author at: McKetta Department of Chemical Engineering, The University of Texas at Austin, Austin, TX 78712, USA.
E-mail address: gshwang@che.utexas.edu (G.S. Hwang).

https://doi.org/10.1016/j.apsusc.2020.148557
Received 10 July 2020; Received in revised form 14 November 2020; Accepted 19 November 2020
Available online 11 December 2020

examine the adsorption and dissociation of CH_3F on the Si_3N_4 surface, particularly the H-terminated N-rich (0001) surface of β-Si_3N_4, using first-principles calculations. We then discuss possible mechanisms for the dissociative chemisorption of CH_3F and analyze how it would influence the chemical nature of the surface layer. Based on these results, we discuss their implications for the potential role of CH_3F exposure in the subsequent processes required to achieve ALE. The theoretical insight we begin to develop here can lend guidance to further efforts for improvement in Si_3N_4 ALE, particularly for precursor and reactor design for high aspect ratio and selective etch processes.

2. Results and discussion

Fig. 1 shows the surface unit cell (left) and the slab used to model the H-terminated N-rich β- Si_3N_4 (1 × 1) surface (right). The (1 × 1) surface has three primary amines ($N^{1°}$), three secondary amines ($N^{2°}$), and one tertiary amine ($N^{3°}$), as well as three fourfold coordinated Si atoms (each coordinated with one $N^{1°}$, two $N^{2°}$, and one $N^{3°}$). Detailed information about the model slab used can be found in a previous work from our group by Hartmann *et al.* [15]. The N-rich surface was chosen over the Si-rich surface to study the CH_3F decomposition due to the fact that of these two, only the former surface exhibits significant reactivity towards CH_3F. The nucleophilic character of the $N^{1°}$ and $N^{2°}$ groups on the N-rich surface leads to Coulombic interactions between these amines and the weakly electrophilic carbon center of CH_3F. Additionally, the H and F atoms of the CH_3F can interact with the N lone pairs and positively polarized surface H atoms, respectively. In contrast, a H-terminated Si surface exhibits no sizable interactions with CH_3F. We confirmed this by calculating the adsorption energy (E_{ads}) of CH_3F on a H-terminated Si surface, and found E_{ads} to be −0.06 eV. Note that the negative value of E_{ads} represents the energy gain upon adsorption, which is given by $E_{ads} = E_{MeF/slab} - (E_{MeF(g)} + E_{slab})$, where $E_{MeF(g)}$, E_{slab}, and $E_{MeF/slab}$ are the total energies of a CH_3F gas molecule, Si_3N_4 slab, and one CH_3F molecule adsorbed on the Si_3N_4 slab, respectively. In comparison, E_{ads} is predicted to be around −0.20 eV on the N-rich surface. Because of the low likelihood of chemical reaction and weak molecular adsorption on the Si-rich surface, the H-terminated N-rich surface was chosen as our model system, despite the fact that there may be many other surface structures at steady state in the etch process.

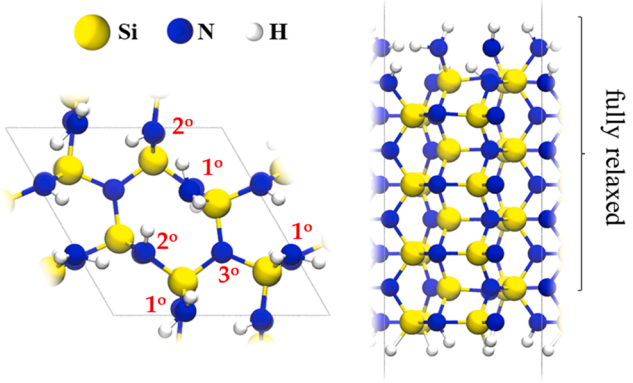

Fig. 1. Top (left) and side (right) views of (0001) β-Si_3N_4 slab used. This slab is constructed by repeating a (1 × 1) unit cell of β-Si_3N_4 4.5 times, generating a 9 layer slab with a N-rich surface; the dangling bonds left by this process are terminated with hydrogen, thereby generating primary ($N^{1°}$) and secondary ($N^{2°}$) groups on the H-terminated N-rich surface. About 15 Å of vacuum above the top surface ensures sufficient vertical separation between periodic images. In our calculations, the bottom layer of Si and N atoms is held fixed and all other atoms in the system are fully relaxed.

2.1. CH_3F adsorption and decomposition

The chemisorption mechanism of CH_3F that we have identified is as follows: first, CH_3F molecularly adsorbs to the Si_3N_4 surface in the configuration shown in Fig. 2(a). Then, as illustrated in Figs. 3 and 4, the backside of the C–F bond is attacked by the lone pair of a neighboring $N^{1°}$ with a somewhat significant energy barrier ($\Delta E^{\ddagger}$) of 0.97 eV, forming an intermediate which quickly proceeds to a final product consisting of an adsorbed F^-/H^+ pair and –$NHCH_3$ moiety; the dissociation of adsorbed CH_3F is predicted to be an exothermic reaction with ΔE_{rxn} = -0.74 eV. The F^-/H^+ pair generated from the dissociative CH_3F adsorption could play a central role in the etching of Si_3N_4.

We begin our analysis with the molecular adsorption of CH_3F. While molecularly adsorbed CH_3F is likely to roam across the SiN surface, we have identified two possible configurations that are particularly energetically favorable, shown in Fig. 2: one [(a)] where CH_3F sits nested in the "hollow" site formed by the three primary amine groups with E_{ads} = −0.20 eV (referred to as Configuration 1), and one [(b)] where CH_3F sits above the surface, with fluorine pointed towards surface H, yielding E_{ads} = −0.21 eV (referred to as Configuration 2).

Our analysis shows that Configuration 1 is well suited for a SN2 reaction; as illustrated in Fig. 3(a), the backside of the C-F bond is well aligned with the nucleophilic lone pair of a surface $N^{1°}$. This nucleophilic attack yields an intermediate state $F^- \cdots -NH_2Me^+$ [(c)] after passing through the transition state [(b)]. The fluoride, although normally not considered an appropriate leaving group for nucleophilic substitution, becomes a better leaving group in this environment due to the stabilizing effects of the hydrogen bonds formed with the two other $N^{1°}$ on the surface, as well as one of the $N^{2°}$ below, each containing electrostatically favorable $H^{\delta+}$, as illustrated in Figure S1. The importance of these groups can be immediately demonstrated by calculating the difference in the energy change (ΔE) for the intermediate formation

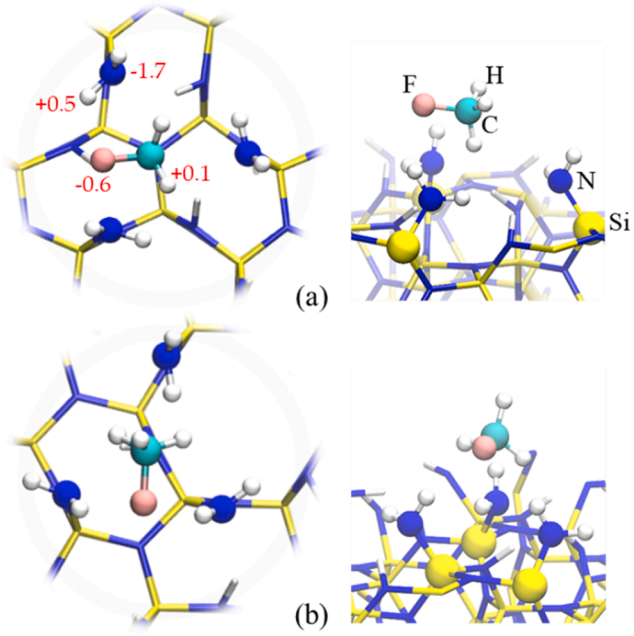

Fig. 2. Two stable configurations 1 [(a)] and 2[(b)] of molecularly adsorbed CH_3F. Left and right panels are top and side views of each configuration, respectively. In Configuration 1 [(a)], the "nested" geometry, CH_3F sits between the three surface $N^{1°}$ groups, with the F approximately equidistant between two adjacent H atoms. Selected Bader charges are shown in red. In Configuration 2 [(b)], the "sitting" geometry, F interacts with surface H atoms and the methyl group can rotate freely above the surface. The CH_3F and nearby $N^{1°}$ groups are drawn as ball and stick, all other atoms in the system are shown as a wireframe. N, Si, H, F, C are shown in blue, yellow, white, pink, and cyan, respectively.

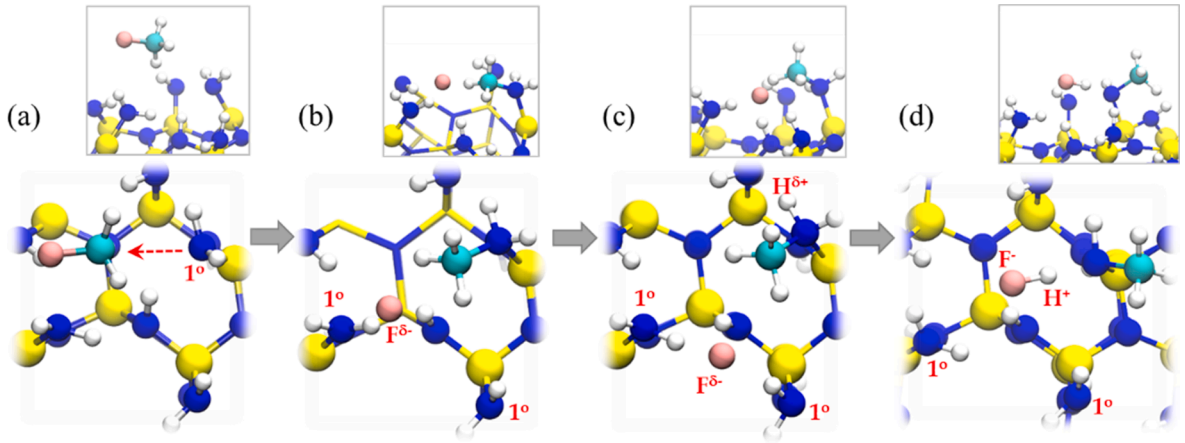

Fig. 3. Reaction pathway of the nucleophilic attack of surface $N^{1°}$ on CH_3F. Beginning with Configuration 1, the lone pair of the primary amine attacks the C-F bond backside, as shown by the arrow ins (a). Proceeding through a transition state (b), F^- is released and stabilized by neighboring H atoms while the C-N bond forms. This results in the intermediate state (c), which quickly forms the final product (d) following rotation of the $–NH_2Me^+$ group and the abstraction of H^+ by F^-. N, Si, H, F, C are shown in blue, yellow, white, pink, and cyan, respectively.

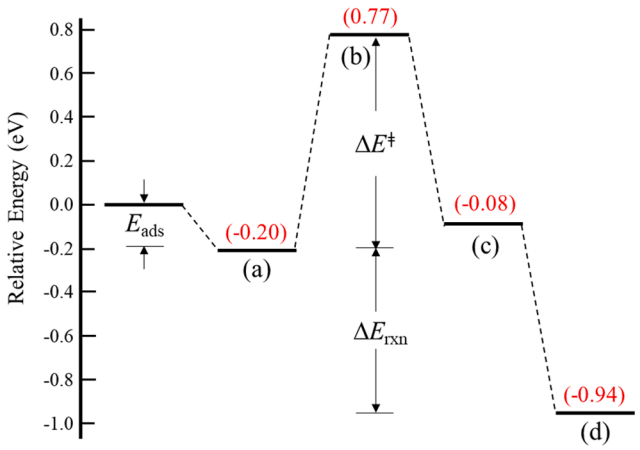

Fig. 4. Energy profile along the reaction pathway for the dissociative chemisorption of CH_3F as shown in Fig. 3.

from the molecularly adsorbed state on a surface with only one $N^{1°}$ (the nucleophile) and the other two $N^{1°}$ replaced with H; the resulting increase of ΔE is about 0.3 eV. Such a surface is illustrated in Figure S2. In contrast to the SN2-like reaction described for Configuration 1, Configuration 2 would require a two-step process (SN1-like) for any reaction to happen with the surface, starting with a cleavage of the C-F bond. Such a step is rather difficult to justify with any chemical intuition. Therefore, all further analysis will be based on a dissociation process starting with the nucleophilic attack of CH_3F in Configuration 1.

After the $N^{1°}$ group attacks the CH_3F, our AIMD simulations show that the formed $–NH_2Me^+$ moiety quickly rotates about the Si–N bond, allowing for the F^- to abstract a proton and form a HF species (illustrated in Figure S3). Note that the HF bond distance (1.11 Å) is actually much larger than the bond length of gas-phase HF (0.94 Å), and thus it could also be considered as an ionic pair (F^-/H^+). By considering the formation of HF as the final product state of the dissociative chemisorption of molecularly adsorbed CH_3F, the predicted ΔE_{rxn} for this process is −0.74 eV, as illustrated in Fig. 4.

We also examined the feasibility of the $N^{2°}$ and $N^{3°}$ sites as nucleophiles for the CH_3F dissociation reaction. The $N^{3°}$ site can be dismissed; not only is it sterically blocked by adjacent $N^{1°}$ and $N^{2°}$ groups, but it lacks the H needed to form the thermodynamically favorable HF product. Furthermore, the ΔE associated with the formation of a methylamine intermediate on this group ($Si_3N–Me^{\delta+}$ — $F^{\delta-}$) is over 2 eV. ΔE associated with the formation of the $–NHMe^+ \cdots F^-$ intermediate on the $N^{2°}$ site is predicted to be 1.1 eV, implying that CH_3F chemisorption is thermodynamically unfavorable on the H-terminated N-rich surface considered in this work. However, this unfavorable ΔE can largely be attributed to steric hindrance generated by neighboring $N^{1°}$ groups in our model system, as ΔE for a sterically unhindered site (Figure S4) is predicted to be 0.10 eV, only a 0.02 eV difference from the ΔE associated with the intermediate formation on $N^{1°}$ groups. Therefore, methylamines may form on $N^{2°}$ sites, followed by proton release to form the final state as seen in Fig. 3; however, we thought explicit consideration of the reactions on $N^{2°}$ sites would not be necessary due to their similarity in nucleophilicity as compared to $N^{1°}$ sites. ΔE values associated with formation of methylamines from each surface group are tabulated in Figure S5(a).

Considering this full pathway, we believe it is relevant to note that the presence of surface hydrogen is important in this process. Not only does H stabilize the F^- — $–NH_2Me^+$ intermediate in the manner described earlier, but it also can be abstracted from $N^{1°}$ and $N^{2°}$ to become a part of a highly reactive HF species, which may play a central role in the etching of SiN.

2.2. Coadsorbate effects

The results presented thus far have suggested that the CH_3F decomposition via this pathway is somewhat unfavorable, both thermodynamically and kinetically. One may wish to consider that these figures were computed using a model of this reaction in isolation on a (2 × 2) slab, which does not account for the effects of coadsorbed molecules and/or products on the nitride surface. In the actual etch process, once can expect other molecules to interact with this system as the reaction progresses. By calculating ΔE for nucleophilic decomposition with each of the configurations shown in Fig. 5, we show that coadsorbates do indeed seem to influence the thermodynamic favorability of this decomposition (Table 1). We note that the presence of any coadsorbate, irrespective of identity, results in significant increases in energetic favorability of the intermediate state and is associated with a decrease in the energy barrier for this dissociative chemisorption reaction. However, we have seen these effects to be quite sensitive to relative geometry of the system, and therefore may influence the reaction energetics quite minimally in reality.

2.3. Coverage effects

The coverage effect of amine methylation was examined by

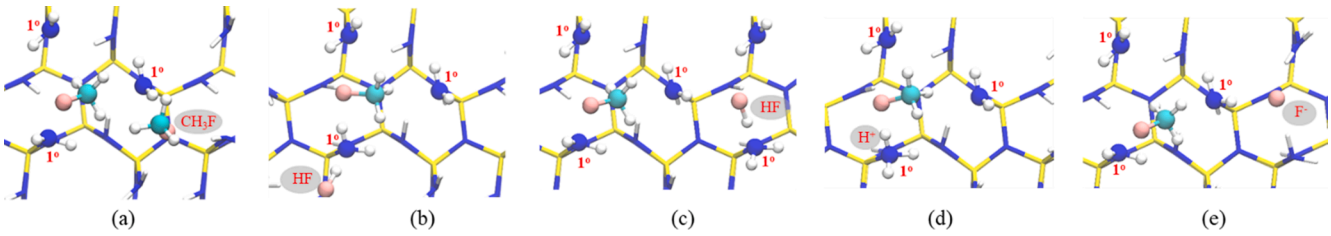

Fig. 5. Coadsorbates, each shown in the configuration used to influence energy barrier ($\Delta E^{\ddagger}$) and reaction energy (ΔE_{rxn}) of the decomposition reaction. Only $N^{1°}$ and CH_3F are shown as ball-and-stick, other atoms are shown as a wireframe. N, Si, H, F, C are shown in blue, yellow, white, pink, and cyan, respectively.

Table 1
Predicted energetics of coadsorbate-assisted dissociation of CH_3F from DFT3-BJ on a (2 × 2) surface supercell.

	None	HF(1)	HF(2)	MeF	F^-	H^+
$\Delta E^{\ddagger}$ (eV)	0.97	0.75	0.70	0.60	0.45	0.31
ΔE (eV)	0.12	−0.23	−0.11	−0.18	−0.53	−0.64

calculating ΔE_{rxn} for the $–NH_2 + CH_3F(g) \rightarrow –NHMe + HF(g)$ reaction at varying coverages of –NHMe, as illustrated in Fig. 6. The predicted ΔE_{rxn} for the methylation of one $N^{1°}$ group out of three per (1 × 1) surface unit cell is −0.08 eV, and it slightly decreases in magnitude to −0.06 eV and −0.03 eV, respectively, for the second and third $N^{1°}$ methylation. The small change in ΔE_{rxn} indicates that the methylation of surface $N^{1°}$ groups can be nearly equally favorable thermodynamically with no significant coverage effect, suggesting that all surface $N^{1°}$ would be converted to –NHMe if CH_3F molecules are sufficiently available. We also considered possible $–NMe_2$ formation from the methylation of –NHMe. The ΔE_{rxn} for the reaction $–NHMe + CH_3F(g) \rightarrow –NMe_2 + HF(g)$ is predicted to be 0.14 eV, energetically less favorable than the methylation of $–NH_2$ due to steric hindrance. Note that here HF in the gas phase is used as the reference state; however, when taking into account the strong adsorption of HF with E_{ads} = -0.89 eV, all the $N^{1°}$ methylation reactions examined can be considered to be quite exothermic. These results imply that a nontrivial fraction of –NHMe could be further be methylated to form $–NHMe_2$, depending on the availability of CH_3F.

3. Implications

According to our calculations, CH_3F may undergo nucleophilic decomposition on the H-terminated N-rich surface, forming reactive HF species (or F^-/H^+ pairs) and methylamine (– NHMe) moieties. However, the results do not fully support the conventional thought that Si_3N_4 ALE involves the removal of a chemically modified surface layer formed by the dissociative chemisorption of CH_3F as reasoned below.

- Even though the N-rich surface considered tends to be the most reactive towards CH_3F, thermal chemisorption is rather unlikely due to the high barrier of 0.97 eV for dissociation of adsorbed CH_3F relative to the energy cost of 0.20 eV for its desorption.
- Methylation of surface amines via nucleophilic substitution of CH_3F is found to have only a negligible effect on the surface chemical nature of Si_3N_4.
- Even assuming the thermal chemisorption and etch was thermodynamically feasible, it is stoichiometrically unreasonable due to excessive hydrogen consumption of the reaction and lack of a pathway for silicon removal.
- The generation of reactive HF species (or F^-/H^+ pairs), rather than amine methylation from CH_3F chemisorption, may play a central role in Si_3N_4 ALE.
- Given the above points, the nonequilibrium reaction of physisorbed CH_3F with the underlying surface under Ar^+ bombardment would perhaps be a key process, which is still under investigation.

3.1. Low initial sticking probability

The probability that CH_3F will dissociatively chemisorb to the surface is described by the so-called initial sticking coefficient (S_0), which is given by

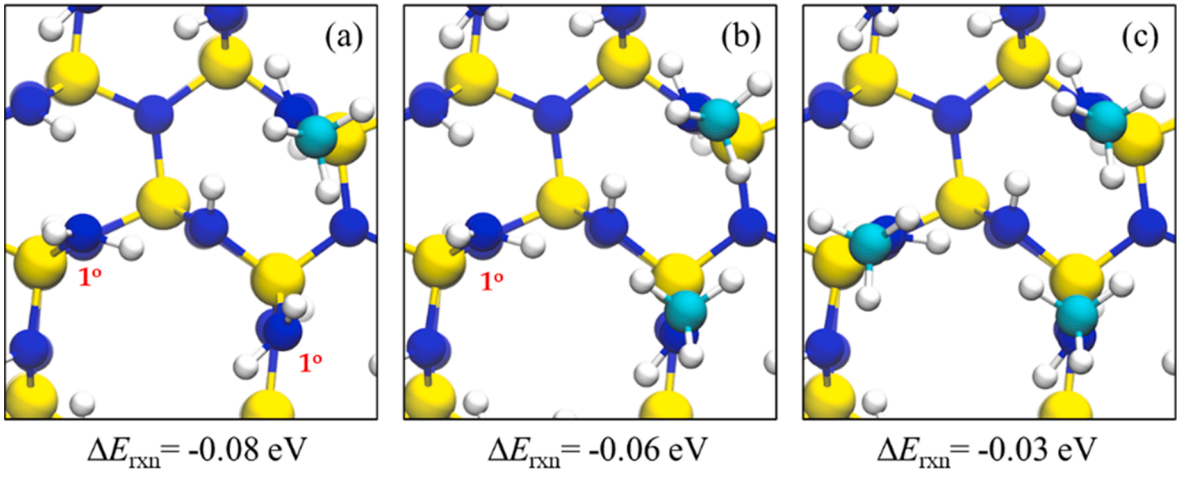

Fig. 6. Surfaces with one (a), two (b), and three (c) methylated $N^{1°}$ groups. For each case, the energy change per methylamine (ΔE_{rxn}) associated with the methylation reaction, i.e., $–NH_2 + CH_3F(g) \rightarrow –NHMe + HF(g)$ is also indicated. N, Si, H, C are shown in blue, yellow, white, and cyan, respectively.

$$S_0 = \frac{k_A}{k_A + k_D} = \frac{\nu_A exp\left(\frac{-E_A}{RT}\right)}{\nu_A exp\left(\frac{-E_A}{RT}\right) + \nu_D exp\left(\frac{-E_D}{RT}\right)} = \frac{1}{1 + \frac{\nu_D}{\nu_A} exp\left(\frac{-(E_D - E_A)}{RT}\right)}$$

where k, Γ, and E are the rate constant, attempt frequency, and energy barrier of the chemisorption (indicated by the subscript A) or desorption (subscript D) of molecularly adsorbed CH_3F, respectively, and R and T refer to the universal gas constant and surface temperature, respectively. Note that $E_D - E_A = (E_{ads} - E^{\ddagger})$ from Fig. 4. Taking $E_A = 0.97$ eV and $E_D = 0.2$ eV, the initial sticking coefficient (S_0) is estimated to be about 1×10^{-11} at $T = 353$ K (the process temperature used by Kim *et al.* [12]) assuming $\Gamma_D = \Gamma_A$. Note that S, the sticking coefficient, will drop with increasing CH_3F coverage. With the influence of coadsorbates, the predicted S_0 would increase, but not necessarily significantly. Most of the barriers listed in Table 1 yield S_0 values around 1×10^{-7}; the lowest barrier possible among the conditions we checked corresponds to the proton coadsorbate and is calculated to be 1×10^{-3}, which is still quite low. As noted earlier, the S_0 values would likely be even lower in reality, due to the influence of coadsorbates being very sensitive to the local environment. Furthermore, Γ_D is generally much greater than Γ_A because of the larger entropy change associated with the physisorption-desorption transition compared to the physisorption-chemisorption transition. Hence, the S_0 of CH_3F can generally be expected to be significantly smaller than 1×10^{-7}, even on what is probably the most reactive surface, as discussed earlier. The very low S_0 suggests that the dissociative chemisorption of CH_3F may hardly occur on any defect-free Si_3N_4 surfaces, thereby resulting in very limited surface chemical modification via CH_3F exposure. Although only one specific model system is considered here, this analysis serves as a good first measure and is well in line with other reasons below for our claim that surface chemical modification with CH_3F prior to Ar^+ bombardment may not be the underlying mechanism responsible for Si_3N_4 ALE.

3.2. Negligible surface chemical modification

The effect of N^{1° methylation on the chemical nature of the surface was examined by assessing the methylation-induced change in the Si-N bond strength via calculation of the stretching frequency of various Si-N bonds on the surface. The vibrational frequency (ν) is directly related to the bond energy (E), i.e., $E \propto h\nu$ where h is Planck's constant; hence, a lower vibrational frequency can be assumed to be a weaker bond. The Si-N stretching frequency of N^{1° (Si-NH_2) is calculated to be 1114 cm^{-1}, and decreases only by 30 cm^{-1} upon methylation (Si-NHMe). Furthermore, the Si-N bond length and occupancy increase only by about 0.01 Å and 0.02*e* respectively. Even when all surface N^{1° groups are methylated, we obtained changes of less than 100 cm^{-1} in ν of all Si-N bonds in the surface layer. These results suggest that the amine methylation does not have much of an effect in terms of weakening the surface layer. The insignificant change in chemical nature of the Si_3N_4 surface is further supported by the nearly equal ΔE_{rxn} of −0.52 and −0.54 eV for the reactions Si-NH_2 + HF(g) → SiF + NH_3(g) and Si-NHMe + HF(g) → SiF + NH_2Me(g), respectively. Our analysis leads to speculation that amine methylation itself does not facilitate Si_3N_4 ALE via surface chemical modification.

3.3. Stoichiometric challenges

Although the removal of surface amines via CH_3F is thermodynamically favorable, the resulting F-terminated Si-rich surface is fairly unreactive towards CH_3F. Therefore, a similar mechanism cannot be used for the Si-rich layer removal. Additionally, the thermal mechanism considered here produces H_2NMe and $HNMe_2$, which cannot be the true mechanism due to a net loss of hydrogen for both products. Furthermore, the net equation for the thermal removal of Si_3N_4 with only CH_3F is Si_3N_4 + 12 CH_3F → 3 SiF_4 + 4 NMe_3, due to the fact that thermally, CH_3F can only reasonably dissociate into methyl and fluoride groups. Such a process, while stoichiometrically reasonable, is unlikely to occur because of two primary reasons. Firstly, a single N site becomes less likely to act as a nucleophile as bulky CH_3F groups are added. Thus, it is highly unlikely that any amine group will accommodate any more than two methyl groups. Secondly, with only two methyl fluoride molecules reacted per N atom, fully coordinating all Si atoms in the top layer with F would not be possible. With no thermodynamically feasible full etch mechanism, it is apparent that the Ar^+ bombardment must be a key component to the ALE process, perhaps through nonequilibrium formation of such products as HN=CH_2. Our recent preliminary work has demonstrated that Ar^+ bombardment helps achieve a large number of effects in a methylated Si_3N_4 system in the presence of reactive HF species, and allows for nonequilibrium processes to occur. The results will be presented elsewhere.

3.4. Reactive HF species generation and its critical contribution

Reactive HF species (and/or F^-/H^+ pairs) can be generated from CH_3F decomposition via either thermal chemistry or Ar^+ ion bombardment. As presented earlier, the desorption of a HF species to be an endothermic reaction, with a predicted endothermicity of 0.89 eV on the H-terminated N-rich Si_3N_4 surface. This suggests that the HF species produced would favorably remain on the surface and may subsequently be involved in Si-N bond cleavage reactions in which Si-F and N-H bonds are formed with Si-N bond scission. Similar behavior of H and F is expected in chemical wet etching of Si_3N_4 in HF aqueous solution [14,16]. In addition, a recent work by Sherpa *et al.* [17] showed that etching of Si_3N_4 could be achieved with alternating steps of H and F plasma, further demonstrating that these two species can be major contributors to Si_3N_4 ALE under not only thermal but also athermal conditions. The details of the reaction dynamics of HF species (and/or F^-/H^+ pairs) will be discussed in further work to come; nonetheless, our work suggests that CH_3F largely serves to be a self-limiting source of reactive HF species (or F^-/H^+ pairs), rather than being the main etchant.

3.5. CH_3F physisorption and the role of Ar^+ bombardment

Considering the very low S_0 of CH_3F, the bombardment of physisorbed CH_3F with Ar^+ may be a major contributor to Si_3N_4 ALE, particularly when the surface contains a low density of dangling bonds. The E_{ads} of physisorbed CH_3F at low coverage is −0.21 eV, and slightly increases in magnitude to −0.23 eV on average when monolayer saturation, 3 CH_3F per (1 × 1) unit cell, is reached. The E_{ads} for CH_3F physisorbed on top of the first adsorption layer is only −0.04 eV, suggesting that the formation of a bilayer is not particularly favorable. With a monolayer of physisorbed CH_3F, Ar^+ ion bombardment may induce a wide variety of activated processes. Perhaps most crucially, such low-energy (20–50 eV) ion bombardment can induce the release of fluoride via cleavage of the C-F bond in CH_3F, a result repeatedly observed in our AIMD simulations (Figure S6). These preliminary AIMD simulations have shown that a variety of processes can also occur through this bombardment, such as N-C bond formation, creation of dangling bonds, and general disruption of crystal structure at the surface (Figure S7). Characterization of the effects of such processes, both instantaneous and quasi-equilibrium states, will be critical to understanding the full ALE process, particularly for tuning these processes to yield high-quality films. It may be possible that chemical modification of SiN surfaces can primarily be achieved via fluorocarbon fragments interacting with highly reactive structural defects and highly strained bonds as generated via ion bombardment. Detailed investigation of Ar^+ bombardment-induced nonequilibrium processes is ongoing and will be described in further work to come.

4. Summary

This work examined possible mechanisms for the dissociative chemisorption of CH_3F on Si_3N_4 and analyzed its influence on the chemical nature of the surface using first-principles DFT calculations. Here, we only considered the H-terminated N-rich surface of (0001) β-Si_3N_4 that tends to be the most reactive towards CH_3F. The most likely mechanism begins with the molecular adsorption of CH_3F with an exothermicity of E_{ads} = -0.2 eV. A primary amine ($N^{1°}$), acting as a nucleophile, attacks the C in CH_3F, accompanied by the release of F, to form an intermediate F^- — –NH_2Me + complex; the associated activation barrier $\Delta E^{\ddagger}$ and energy change ΔE are predicted to be 0.97 eV and 0.1 eV, respectively. The intermediate quickly rearranges to form a reactive HF species and –NHMe, yielding ΔE_{rxn} = -0.74 eV for the dissociation reaction of adsorbed CH_3F. Our calculations also show that the reaction energetics would be sensitive to the local surface environment. Firstly, ΔE_{rxn} significantly decreases in magnitude in the absence of adjacent $N^{1°}$ groups that stabilize the released F^-. Secondly, both $\Delta E^{\ddagger}$ and ΔE can decrease substantially in the presence of coadsorbates that help stabilize the transition state as well as the intermediate F^- — -NH_2Me^+ complex.

Based on this mechanism, the potential role of CH_3F chemisorption in Si_3N_4 ALE was evaluated. First, the initial sticking probability S_0 was estimated to have an upper bound of 1×10^{-11} under the conditions considered, at a typical ALE temperature ($T = 353$ K); this implies that the dissociative chemisorption of CH_3F, even on this most active surface of Si_3N_4, is quite unlikely to happen thermally. The sticking probability may increase in the presence of stabilizing coadsorbates, but generally only to values around 1×10^{-7}, a relatively insignificant increase in probability. Second, the methylation of surface amines has minimal impact on the surface chemical nature, weakening Si-N bonds by less than 100 cm^{-1} regardless of the degree of surface methylation. Third, such a mechanism is stoichiometrically unreasonable, due to the unsustainable consumption of H and a lack of explainable Si layer etch. This analysis suggests that the ALE of Si_3N_4 with CH_3F may not follow the generally accepted mechanism involving surface chemical modification via CH_3F exposure, especially when the SiN surface contains a low density of dangling bonds. Instead, we propose that reactive HF species (or F^-/H^+ pairs), potentially generated from CH_3F dissociation induced by Ar^+ bombardment, could be the primary etchants like in Si_3N_4 etching with HF solutions. Our work highlights the potentially critical role played by Ar^+ bombardment in not only removing material but also causing dissociation of molecularly adsorbed CH_3F and surface activation. This may warrant further studies on the ion bombardment-induced nonequilibrium processes to better understand and optimize the Si_3N_4 ALE process.

5. Computational methods

Density functional theory (DFT) calculations using the generalized gradient approximation (GGA) were performed using the Vienna Ab initio Simulation Package (VASP) [18]. The Perdew-Burke-Ernzerhof (PBE) functional [19] was used to describe exchange–correlation energies, and the projector augmented wave (PAW) method [20] was used to describe the interaction between ion core and valence electrons. The Kohn-Sham orbitals were expanded in a plane wave basis set with a cutoff energy of 450 eV and a Γ-centered 2 × 2 × 1 k-point mesh was used to sample the Brillouin zone. The periodic (2 × 2) slab model was used in this work, except where otherwise noted. Atomic partial charges were calculated using Bader charge analysis [21] as implemented in VASP, with core and valence electron density accounted for by integration over the simulation cell. Reaction barriers were evaluated with the climbing image nudged elastic band method (CI-NEB) [22] with 5 images per calculation and a spring constant of 5.0 eV/Å^2. All DFT calculations were performed with the van der Waals dispersion correction method of Grimme with Becke-Johnson damping, also known as DFT-D3BJ [23,24]. Ab initio molecular dynamics (AIMD) simulations were performed within the Born-Oppenheimer approximation with a time step of 1 fs and a Nosé-Hoover thermostat; here, an energy cutoff of 350 eV and Γ point sampling were used. Visualizations were generated using VMD [25].

CRediT authorship contribution statement

Erik Cheng: Investigation, Writing - original draft. **Gyeong S. Hwang:** Conceptualization, Writing - review & editing.

Declaration of Competing Interest

The authors declare that they have no known competing financial interests or personal relationships that could have appeared to influence the work reported in this paper.

Acknowledgements

This work was supported by Tokyo Electron Limited (TEL) and the R. A. Welch Foundation (No. F-1535). We would like to thank Dr. Peter Ventzek and Dr. Alok Ranjan at Tokyo Electron America for the helpful discussions and suggestions and also the Texas Advanced Computing Center for use of the Stampede2 supercomputing system (OCI-1134872).

Appendix A. Supplementary data

Supplementary data to this article can be found online at https://doi.org/10.1016/j.apsusc.2020.148557.

References

[1] K. Schuegraf, M.C. Abraham, A. Brand, M. Naik, R. Thakur, IEEE J. Electron Devices Soc. 1 (2013) 66.
[2] G.M. Moore, Electronics 38 (1965) 114.
[3] K.J. Kanarik, T. Lill, E.A. Hudson, S. Sriraman, S. Tan, J. Marks, V. Vahedi, R. A. Gottscho, J. Vac. Sci. Technol., A 33 (2015), 020802.
[4] K.J. Kanarik, S. Tan, R.A. Gottscho, J. Phys. Chem. Lett. 9 (2018) 4814.
[5] G.S. Oehrlein, R. Tromp, J. Tsang, Y. Lee, E. Petrillo, Journal of The Electrochemical Society 132 (1985) 1441.
[6] S.W. Pang, D.D. Rathman, D.J. Silversmith, R.W. Mountain, P.D. DeGraff, J. Appl. Phys. 54 (1983) 3272.
[7] Yoder, M. N. United States Patent 7413882, 1988.
[8] D. Metzler, C. Li, S. Engelmann, R.L. Bruce, E.A. Joseph, G.S. Oehrlein, J. Chem. Phys. 146 (2017), 052801.
[9] S. Rauf, T. Sparks, P.L. Ventzek, V.V. Smirnov, A.V. Stengach, K.G. Gaynullin, V. A. Pavlovsky, J. Appl. Phys. 101 (2007), 033308.
[10] W.-H. Kim, D. Sung, S. Oh, J. Woo, S. Lim, H. Lee, S.F. Bent, J. Vac. Sci. Technol., A 36 (2018) 01B104.
[11] C.E. Morosanu, Thin Solid Films 65 (1980) 171–208.
[12] M. Gupta, V.K. Rathi, R. Thangaraj, O.P. Agnihotri, K.S. Chari, Thin Solid Films 204 (1991) 77.
[13] Y.V. Barsukov, V. Volynets, A.A. Kobelev, N.A. Andrianov, A.V. Tulub, A. S. Smirnov, J. Vac. Sci. Technol., A 36 (2018), 061301.
[14] D.M. Knotter, N. Stewart, I. Sharp, Solid State Phenom. 103–104 (2005) 103–106.
[15] G. Hartmann, P.L.G. Ventzek, T. Iwao, K. Ishibashi, G.S. Hwang, PCCP 20 (2018) 29152.
[16] Martin Knotter, D.; (Dee) Denteneer, T. J. J. Journal of The Electrochemical Society 2001, 148, F43.
[17] S.D. Sherpa, P.L.G. Ventzek, A. Ranjan, J. Vac. Sci. Technol., A 35 (2017) 05C310.
[18] G. Kresse, J. Furthmüller, Physical Review B 54 (1996) 11169.
[19] J.P. Perdew, K. Burke, M. Ernzerhof, Phys. Rev. Lett. 77 (1996) 3865.
[20] P.E. Blöchl, Physical Review B 50 (1994) 17953.
[21] G. Henkelman, A. Arnaldsson, H. Jónsson, Comput. Mater. Sci. 36 (2006) 354.
[22] G. Henkelman, B.P. Uberuaga, H. Jónsson, J. Chem. Phys. 113 (2000) 9901.
[23] S. Grimme, S. Ehrlich, L. Goerigk, J. Comput. Chem. 32 (2011) 1456.
[24] S. Grimme, J. Antony, S. Ehrlich, H. Krieg, J. Chem. Phys. 132 (2010), 154104.
[25] W. Humphrey, A. Dalke, K. Schulten, J. Mol. Graph. 14 (1996) 33.